scientific reports

Check for updates

OPEN

Cooperative role of MDSCs and Tregs in alum-induced alloimmune tolerance in corneal transplantation

Lifang Li[2], Yuping Han[3], Xiangrong Xie[1], Dakun Ren[1], Ying Zhang[1], Shaofeng Hao[1]✉ & Xuming Guo[1]✉

Alum, a widely used adjuvant, has recently been recognized for its capacity to modulate immune responses beyond classical activation. In this study, we investigated whether alum-induced expansion of myeloid-derived suppressor cells (MDSCs) and their interaction with regulatory T cells (Tregs) promote immune tolerance in corneal transplantation. C57BL/6 mice received repeated intraperitoneal alum injections to induce MDSCs, which were subsequently characterized and tested in suppression assays. Corneal allograft recipients were treated with alum, adoptive transfer of alum-induced MDSCs, or combined transfer of MDSCs and Tregs. Alum significantly expanded MDSCs in the spleen, blood, and bone marrow, and suppressed $CD4^+$ T cell proliferation. Compared with MDSCs transfer alone, alum treatment more effectively prolonged allograft survival (50% vs. 20% tolerance), increased $Foxp3^+$ Tregs and $IL\text{-}10^+$ Treg cells, and reduced Th17 responses. Co-transfer of MDSCs and Tregs further enhanced graft survival (~ 60%), indicating a synergistic effect. These findings suggest that alum enhances transplant tolerance through both expansion and activation of MDSCs and Tregs, providing mechanistic insight into its immunosuppressive potential and offering a rationale for combined cell-based strategies in transplantation.

Keywords Alum, MDSCs, Tregs, Corneal transplantation, Immune tolerance, Allograft survival

Immune modulation is a critical determinant of success in organ transplantation, where the recipient's immune system must be carefully regulated to prevent graft rejection. Among various immunoregulatory populations, myeloid-derived suppressor cells (MDSCs) have gained attention for their capacity to suppress T cell activation and proliferation. MDSCs consist of two main subsets—polymorphonuclear MDSCs (PMN-MDSCs) and monocytic MDSCs (M-MDSCs)—and play established roles in immune suppression in cancer, autoimmunity, and infectious diseases[1–5]. However, their function in the context of alloimmune responses in transplantation remains incompletely understood[6,7].

Alum, a widely used vaccine adjuvant, has recently been shown to promote MDSC expansion in vivo and may offer a novel approach to immune regulation in transplantation[8]. Previous studies have reported that alum enhances the accumulation of MDSCs, suppresses T cell proliferation, and facilitates the development of a tolerogenic immune environment[9]. Nevertheless, whether alum-induced MDSCs alone are sufficient to mediate long-term allograft survival, or whether other regulatory cell types are involved, remains unclear.

In particular, regulatory T cells (Tregs) and IL-10–producing $CD4^+$ T cells are critical for maintaining immune tolerance, yet the potential of alum to modulate these populations has not been fully explored. Previous studies have demonstrated that in vitro–generated MDSCs are capable of suppressing neovascularization and immune rejection in murine corneal transplantation models[10–13]. Building on these findings, the present study aimed to explore a novel strategy for inducing the in vivo expansion of MDSCs using the adjuvant alum, and to evaluate its efficacy in preventing immune-mediated rejection in corneal allografts. This raises the possibility that alum may contribute not only to the expansion of MDSCs but also to the activation of Tregs, thereby enhancing their therapeutic potential[14].

[1]Department of Ocular Surface and Refraction, Heji Hospital Affiliated to Changzhi Medical College, 161 East Jiefang Road, Changzhi 046000, Shanxi, PR China. [2]Department of Respiratory and Critical Care Medicine, The Second Hospital of Shanxi Medical University, Taiyuan 030001, Shanxi, PR China. [3]Department of Ocular Surface Diseases, The Shanxi Eye Hospital, Taiyuan 030001, Shanxi, PR China. ✉email: hejiyanke@sina.com; Guoxuming1124@163.com

In this study, we sought to determine the relative contribution of alum-induced MDSCs and Tregs to immune tolerance in a murine corneal transplantation model. Specifically, we compared the effects of alum administration, adoptive transfer of alum-induced MDSCs, and combined transfer of MDSCs and Tregs on allograft survival. Flow cytometric analysis was used to characterize immune cell subsets—including Th1, Th17, Tregs, and $CD4^+IL\text{-}10^+$ regulatory T cells—in the draining lymph nodes of graft recipients. We hypothesized that alum promotes corneal graft survival not only by expanding MDSCs but also by activating Tregs, leading to a broader and more durable immunosuppressive effect. This study aims to provide novel insights into the mechanisms of alum-mediated immune regulation and offers a potential combinatorial strategy for enhancing transplant tolerance.

Results

Expansion of MDSCs by alum

To investigate the expansion of MDSCs in alum-treated mice, $CD11b^+Gr1^+$ cells were analyzed in the spleen (SP), blood, and bone marrow (BM). The frequencies of $CD11b^+Gr1^+$ cells increased from 1.2 to 8.5% in the spleen, from 23.8 to 60.2% in the bone marrow, and from 6.6 to 35.8% in the blood following alum administration (Fig. 1A,B).

Phenotypic analysis of these cells by flow cytometry revealed that, compared to PBS-treated controls, alum-induced MDSCs exhibited increased expression of Ly6C and Ly6G. $Ly6C^{low}Ly6G^+$ cells constituted 66.3% of $CD11b^+Gr1^+$ cells in the bone marrow and 67.7% in the spleen, while $Ly6C^+Ly6G^-$ cells constituted 32.6% and 28.0%, respectively. These findings indicate that alum-induced MDSCs include both PMN-MDSCs ($CD11b^+Ly6C^{low}Ly6G^+$) and M-MDSCs ($CD11b^+Ly6C^+Ly6G^-$) subpopulations. The expression levels of CD80, CD86, CD40, TLR4, TLR2, and MHC-II were similar between alum-treated and PBS-treated groups (Fig. 1C). Phenotypic analysis showed that alum-induced MDSCs exhibited low expression of key co-stimulatory and activation markers, including CD80, CD86, MHC-II, CD40, TLR4, and TLR2. This suggests that alum maintains MDSCs in an immature, non-inflammatory state, preventing their differentiation into functionally mature antigen-presenting cells (APCs).

Functional analysis of $CD11b^+Gr1^+$ cells in alum-induced mice

To assess the immunosuppressive function of alum-induced MDSCs on $CD4^+$ T cells, $CD11b^+$ cells were co-cultured with $CD4^+$ T cells at different ratios. At a $CD11b^+$:T cell ratio of 1:2, a 46.4% suppression of $CD4^+$ T cell

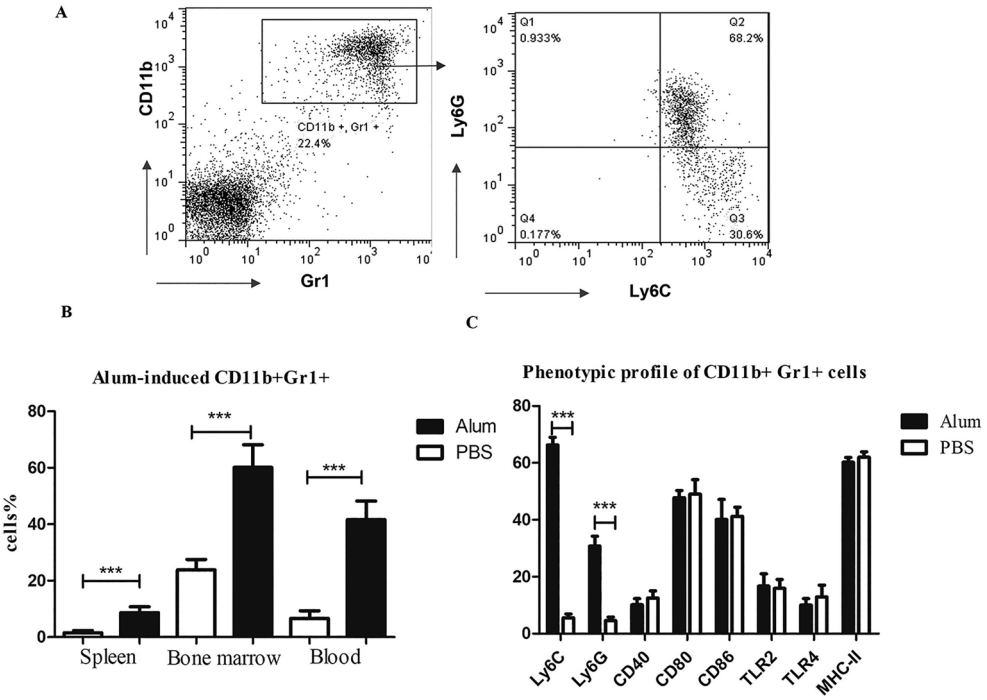

Fig. 1. Alum-induced MDSCs expansion and phenotypic characteristics. (**A**) Respresentative flow cytometry plot showing the gate strategy for $CD11b^+Gr1^+$ MDSCs in speen of alum-treated mice. (**B**) Quantification of $CD11b^+Gr1^+$ MDSCs in spleen, bone marrow, and blood of PBS-and alum-treated mice.Alum administration significantly increased the proportion of MDSCs in all three compartments. $^{***}P < 0.001$. (**C**) Flow cytometry analysis of MDSC subsets based on Ly6G and Ly6C expression. PMN-MDSCs ($CD11b^+Ly6G^+Ly6C^{low}$) and M-MDSCs ($CD11b^+Ly6G^-Ly6C^+$) were identified. (**D**) Phenotypic characterization of $CD11b^+Gr1^+$ MDSCs, showing the expression levels of Ly6C, Ly6G, CD40, CD80, CD86, TLR2, TLR4, and MHC-II in PBS- and alum-treated groups. Alum treatment resulted in a significant increase in $Ly6C^+$ and $Ly6G^+$ cells. $^{***}P < 0.001$. Data are presented as mean ± SD, and statistical significance was determined using an unpaired t-test.

proliferation was observed. At a 1:8 ratio, suppression was 12.1%, while no significant effect was observed at a 1:16 ratio or in control mice. No significant differences were observed between alum-induced SP-MDSCs and BM-MDSCs in their ability to suppress T cell proliferation across different ratios (Fig. 2A,B).

Further analysis revealed that alum-induced MDSCs downregulated CD25 and CD40L expression by 33.3% and 44.3%, respectively, while upregulating PD-1 and Foxp3 by 16.0% and 318.3%, respectively as shown in Fig. 2C. No significant changes were observed in CD69, PD-L1, CD62L, or CTLA-4 expression (Table 1, -supplementary material). These findings suggest that alum-induced MDSCs function as immunosuppressive cells, effectively inhibiting T cell proliferation and activation while promoting Foxp3 expression.

Suppression of corneal allograft rejection by alum and alum-induced MDSCs

To evaluate the immunosuppressive effects of alum and alum-induced MDSCs on corneal allograft survival, we performed following BALB/c-to-C57BL/6 corneal transplantation.As shown in Fig. 3A, mice receiving allogeneic grafts with PBS treatment (PBS group) exhibited rapid rejection, with complete graft failure observed by day 13 post-transplantation. In contrast, alum-treated recipients demonstrated significantly improved graft survival, with approximately 50% of grafts remaining clear and accepted beyond day 30 ($p = 0.0005$ vs. allogeneic control). Syngeneic grafts were uniformly accepted, maintaining 100% survival throughout the observation period.

Based on the observed results, we hypothesized that alum-induced MDSCs are the primary mediators of the immunosuppressive effects observed following alum treatment. To test this, we performed adoptive transfer of alum-induced MDSCs as a therapeutic intervention in the murine corneal transplantation model. The alum group showed a significantly improved allograft survival rate compared to the MDSCs group and PBS group ($p = 0.0042$). The survival rate in the MDSCs group was higher than that in the PBS group ($p = 0.0429$). The treatment outcomes revealed that approximately 50% of allogeneic corneal grafts in the alum-treated group and 20% in the alum-induced MDSCs group achieved permanent tolerance (Fig. 3B). These results suggest that both alum and alum-induced MDSCs adoptive transfer have immune-suppressive functions in corneal alloreaction.

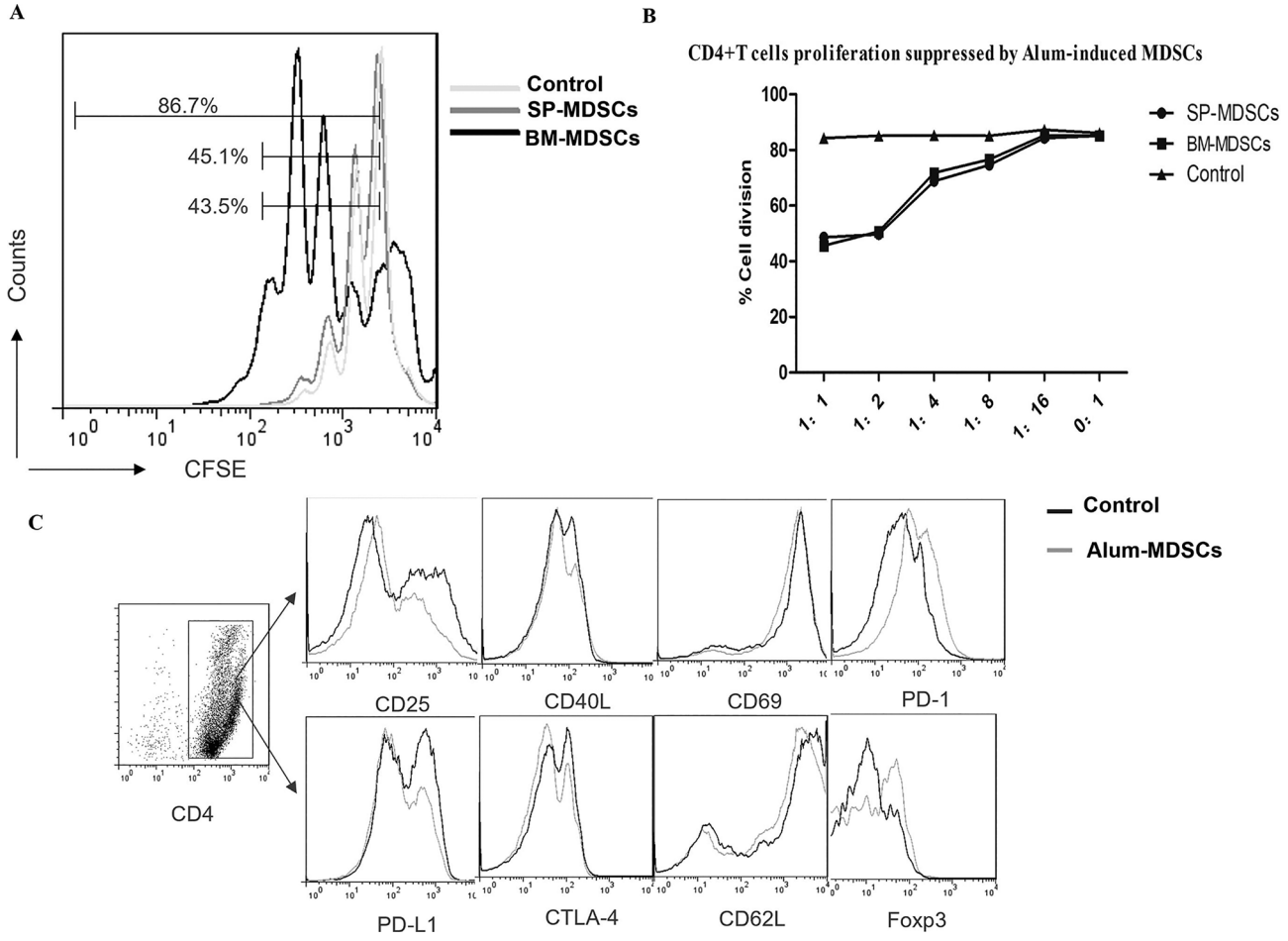

Fig. 2. Suppressive function of alum-induced MDSCs on $CD4^+$ T cell proliferation. (**A**) Representative CFSE dilution assay demonstrating the suppressive effect of MDSCs on $CD4^+$ T cell proliferation. $CD4^+$ T cells were labeled with CFSE and stimulated with anti-CD3/CD28 in the presence or absence of MDSCs. The percentage of proliferating cells is indicated. (**B**) Quantification of T cell division in the presence of SP-MDSCs and BM-MDSCs at different MDSC-to-T cell ratios. Both SP-MDSCs and BM-MDSCs exhibited a dose-dependent suppression of T cell proliferation.Data are presented as mean ± SD.

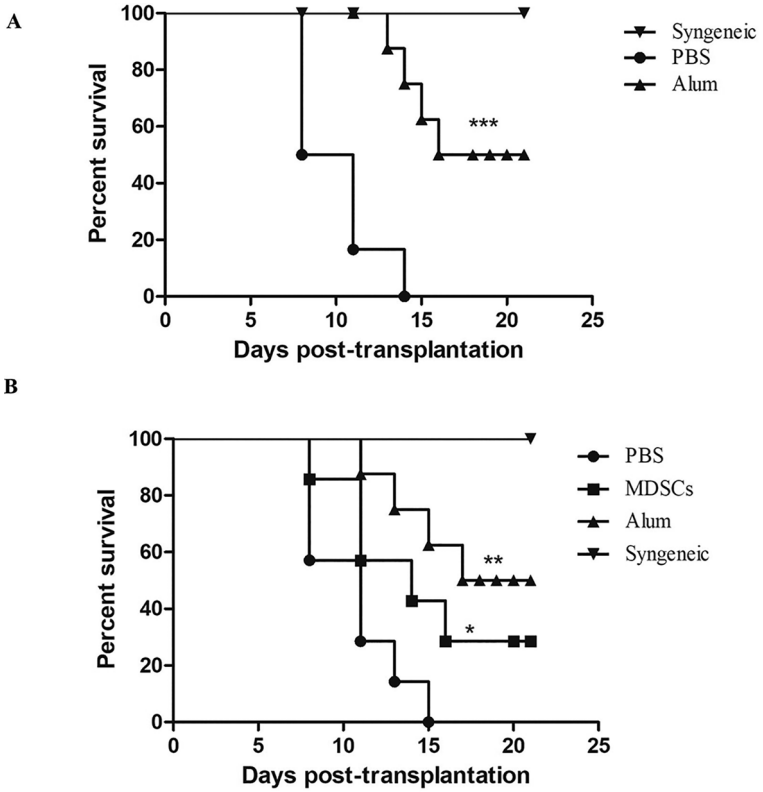

Fig. 3. Alum-induced MDSCs improve corneal allograft survival. (**A**) Alum-treated mice showed significantly prolonged corneal allograft survival compared to untreated allogeneic controls. Approximately 50% of the alum-treated recipients maintained long-term graft clarity, while all allogeneic controls experienced complete rejection within 15 days (**B**) Comparison of graft survival in PBS-treated, alum-treated, MDSC-treated, and syngeneic control groups. Alum treatment significantly improved graft survival compared to PBS and MDSC groups, while MDSC transfer alone resulted in moderate prolongation. Syngeneic grafts remained fully accepted without signs of rejection throughout the observation period. Statistical significance was assessed using the log-rank test. $^{***}p < 0.001$;$^{**}p < 0.01$; $^{*}p < 0.05$.

Alum-induced tregs could not be reproduced by MDSCs adoptive transfer

To elucidate the mechanisms underlying the treatment differences between the alum group and the alum-induced MDSCs group, we extracted draining lymph nodes (LNs) from mice for cytokine and Foxp3 analysis. The results showed that alum treatment led to an increase in the percentage of $CD4^+CD25^+Foxp3^+$ cells to 42.8%, while the percentage in the alum-induced MDSCs group was 25.8%, and 27.6% in the PBS group, 24.8% in the control group ($p = 0.0023$), as shown in Fig. 4A,B. There was no significant difference in Foxp3 expression levels between the MDSCs group, PBS group, and control group ($p = 0.810$).

Since allogeneic corneal transplant rejection depends on the balance between Th1, Th17, Treg, and $CD4^+IL\text{-}10^+$ regulatory T cells, we further analyzed their proportions. The results showed that $CD4^+IL\text{-}2^+$ T cells were 18.5% in the PBS group, while the corresponding percentages were 4.5% in the alum group, 4.8% in the alum-induced MDSCs group, and 1.6% in the control group ($p < 0.001$). The percentage of $CD4^+IL\text{-}2^+$ T cells showed no difference between the alum group and the alum-induced MDSCs group ($p = 0.6482$). $CD4^+IFN\text{-}\gamma^+$ T cells were 1.0% in the PBS group, while the corresponding percentages were 0.4% in the alum group, 0.45% in the alum-induced MDSC group, and 0.31% in the control group ($p < 0.001$). The percentage of $CD4^+$ $IFN\text{-}\gamma^+$ T cells showed no difference between the alum group and the alum-induced MDSCs group ($p = 0.5065$). $CD4^+IL\text{-}17\ A^+$ T cells were 1.5% in the PBS group, while the corresponding percentages were 0.34% in the alum group, 1.2% in the alum-induced MDSC group, and 0.2% in the control group ($p = 0.0002$). The percentage of $CD4^+IL\text{-}17\ A^+$ T cells showed no difference between the PBS group and the alum-induced MDSCs group ($p = 0.3171$). $CD4^+IL\text{-}10^+$ T cells were 3.5% in the PBS group, while the corresponding percentages were 5.3% in the alum group, 3.5% in the alum-induced MDSCs group, and 0.2% in the control group ($p = 0.0182$). The percentage of $CD4^+IL\text{-}10^+$ T cells showed no difference between the PBS group and the alum-induced MDSC group ($p = 0.9186$), as shown in Fig. 4C.

These results indicate that both alum and alum-induced MDSCs adoptive transfer had similar effects in suppressing Th1 cells but not Th17 cells. However, alum showed a stronger ability to induce Treg and $CD4^+IL\text{-}10^+$ regulatory T cells expansion in alloimmune reactions. Treg cells play a crucial role in maintaining immune tolerance and preventing graft rejection. This may explain the higher proportion of permanent graft tolerance in the alum-treated group.

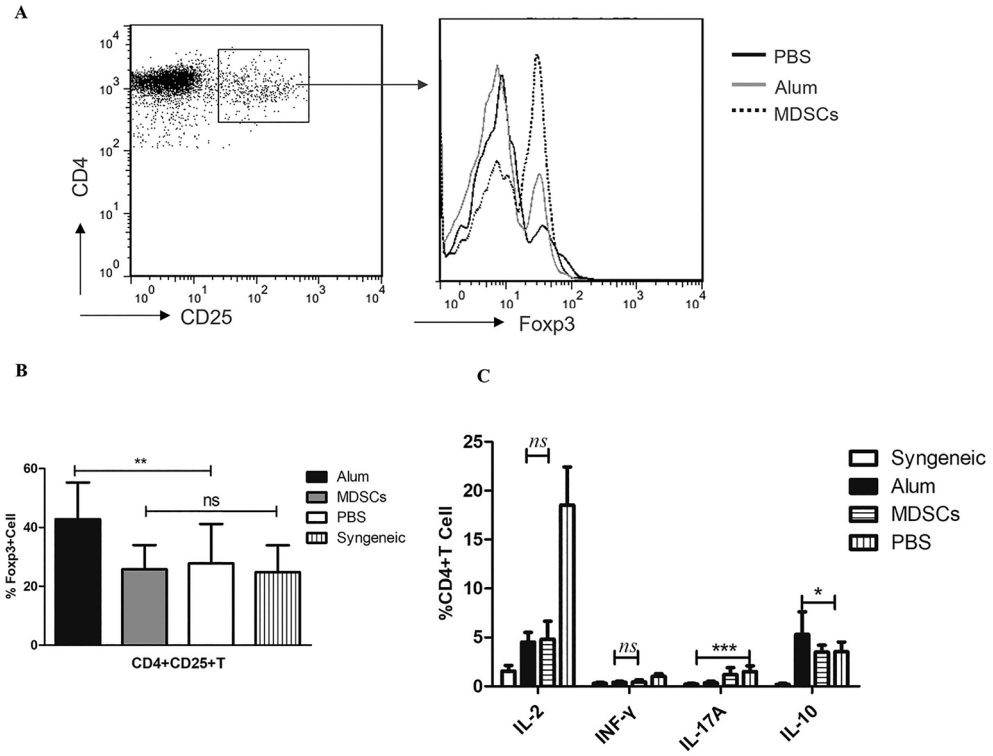

Fig. 4. Alum-induced MDSCs modulate T cell responses in corneal allograft recipients. (**A**) Representative flow cytometry plots showing the percentage of Treg cells in the draining lymph nodes of corneal allograft recipients across different treatment groups (Alum, MDSCs, and PBS). (**B**) Quantification of Foxp3⁺ Tregs as a percentage of CD4⁺ T cells in different treatment groups. Alum-treated mice exhibit a significantly higher proportion of Tregs compared to PBS-treated controls ($^{*}p < 0.05$), while no significant difference (ns) is observed between MDSC-treated and PBS-treated groups. (**C**) Cytokine profiling of CD4⁺ T cells from draining lymph nodes. Alum treatment significantly reduces pro-inflammatory cytokines IL-2, IFN-γ, and IL-17 A, while increasing IL-10, an immunoregulatory cytokine. Statistical significance: $^{***}p < 0.001$, $^{**}p < 0.01$, $^{*}p < 0.05$.

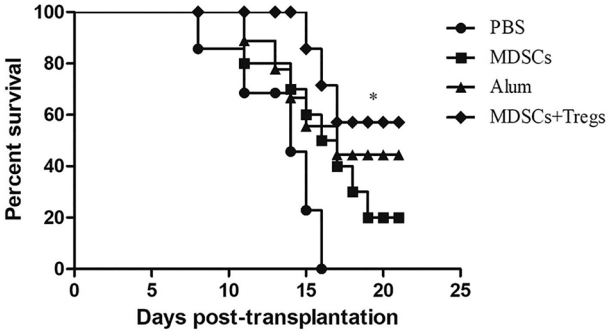

Fig. 5. Kaplan–Meier survival curves of corneal allografts in different treatment groups. C57BL/6 mice receiving BALB/c corneal allografts were treated with either alum, adoptive transfer of MDSCs, co-transfer of MDSCs and Tregs, or no treatment (allogeneic control). Graft survival was monitored for 21 days post-transplantation.

Combined transfer of MDSCs and Tregs further enhances corneal allograft survival

To investigate whether the limited immunosuppressive effect of adoptively transferred MDSCs could be enhanced by regulatory T cells (Tregs), we performed co-transfer of alum-induced MDSCs and Tregs into C57BL/6 recipients of BALB/c corneal allografts.

As shown in Fig. 5, recipients of combined MDSCs + Tregs displayed significantly prolonged graft survival compared to either MDSCs or alum monotherapy. Approximately 60% of grafts remained clear and survived beyond day 30 in the MDSCs + Tregs group, compared to ~ 50% in the alum group and ~ 20% in the MDSCs-

only group. The MDSCs + Tregs group showed a improved allograft survival rate compared to the MDSCs group and PBS group ($p = 0.04$, $p = 0.0024$). Corneal grafts in the alum-treated and MDSCs + Tregs groups remained clear, with no signs of rejection, whereas grafts in the MDSC-only group appeared hazy and partially opaque, indicative of ongoing immune rejection. In contrast, the allogeneic control group exhibited rapid and complete graft rejection (as shown in Fig. 6).

These results suggest a synergistic immunosuppressive effect between MDSCs and Tregs, indicating that Tregs are a necessary component of long-term immune tolerance that cannot be fully replicated by MDSCs transfer alone. This supports the hypothesis that the superior efficacy of alum treatment in promoting allograft tolerance may stem from its ability to simultaneously expand both MDSCs and Treg populations in vivo.

Discussion

MDSCs have been widely recognized for their role in immune modulation across various pathological conditions, including cancer, autoimmunity, and transplantation[15–19]. Their immunosuppressive mechanisms involve diverse pathways, such as metabolic enzyme activity, reactive oxygen species production, secretion of immunoregulatory cytokines, and cell–cell interactions mediated by molecules like PD-L1[20–24]. Although MDSCs have been explored as a potential therapeutic tool in transplantation, their precise contribution to the regulation of alloimmune responses remains incompletely understood.

Although alum is conventionally used as an adjuvant to stimulate immune responses—particularly by activating antigen-presenting cells (APCs)—our results reveal an unexpected immunoregulatory role for this agent. We found that repeated alum injections did not enhance immune activation, but rather suppressed it, establishing a tolerogenic microenvironment. This condition preserved MDSCs in an immature, suppressive state and prevented their differentiation into mature myeloid lineages.

In this study, we investigated the immunomodulatory potential of alum-induced MDSCs in a murine corneal transplantation model. Both alum treatment and adoptive transfer of alum-induced MDSCs significantly prolonged allograft survival. However, the protective effect of alum was clearly superior: approximately 50% of grafts achieved permanent acceptance, compared to only 20% in the MDSC-treated group. These results suggest that, although alum-induced MDSCs exert suppressive effects on alloimmunity, alum itself likely initiates additional immunoregulatory pathways beyond MDSC expansion.

To elucidate these mechanisms, we analyzed immune cell subsets in the draining lymph nodes of transplanted mice. Alum treatment significantly increased the frequency of $CD4^+CD25^+Foxp3^+$ regulatory T cells (Tregs) and $IL\text{-}10^+$ $CD4^+$ T cells, whereas MDSC transfer failed to induce a comparable regulatory expansion. Moreover, only alum—but not MDSCs—effectively suppressed Th17 responses. Although MDSCs are capable of inducing Tregs in vitro, our data suggest that this function is inadequate in vivo without a supportive immunological microenvironment. These observations are consistent with prior reports indicating that Treg induction and stability by MDSCs require additional cues from APCs or stromal cells[25–29].

To further investigate the role of Tregs in this regulatory axis, we conducted a co-transfer experiment involving MDSCs and Tregs. Strikingly, this combination significantly enhanced graft survival compared to either cell type alone, with nearly 60% of grafts achieving long-term acceptance. This synergistic effect supports the hypothesis that Tregs are indispensable partners of MDSCs in establishing durable immune tolerance, and that the limited efficacy of MDSCs alone may stem from the absence of sufficient Treg support. Importantly, in our previous study[14] we showed that adoptively transferred natural Tregs (nTregs) were ineffective in preventing corneal allograft rejection unless functionally activated in vivo. The current findings suggest that alum not only expands but also activates Tregs, thereby enhancing their immunosuppressive function and contributing to improved allograft survival.

Taken together, these findings highlight the multi-faceted immunomodulatory capacity of alum in corneal transplantation. While MDSCs play a significant role in suppressing immune responses, the establishment and

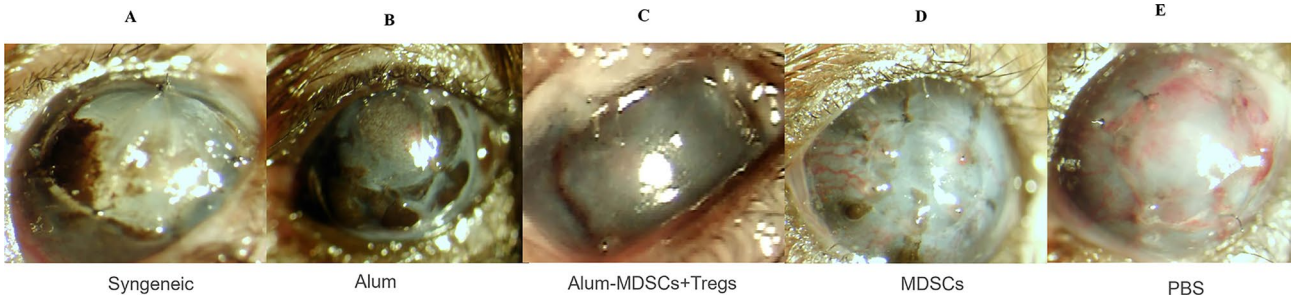

Fig. 6. Representative anterior segment images of corneal grafts on day 21 post-transplantation. Gross photographs of corneal grafts in each experimental group: syngeneic control (**A**), alum-treated (**B**), alum-induced MDSCs combined with Tregs (MDSCs + Tregs) (**C**), MDSCs alone (**D**), and PBS-treated allogeneic controls (E).Corneal grafts in the alum-treated and MDSCs + Tregs groups remained clear, with no signs of rejection. In contrast, the MDSC-only group exhibited partial opacity and mild neovascularization, consistent with ongoing immune rejection. The PBS-treated allogeneic group showed complete graft opacity, edema, and extensive neovascularization, indicating rapid and severe rejection. The syngeneic group maintained full graft clarity as expected.

maintenance of a tolerogenic environment—particularly through Treg expansion and activation—appear to be essential for long-term graft acceptance. This may explain why increasing the dose or frequency of MDSC transfer did not yield improved outcomes, and it underscores the need for combinatorial approaches to replicate the comprehensive immune conditioning achieved by agents like alum. A limitation of this study is the lack of control groups using MDSCs or MDSCs + Tregs isolated from untreated (wild-type) mice, which would help distinguish the specific immunological features conferred by alum induction. Additionally, this study did not examine the in vivo migration patterns of adoptively transferred MDSCs or Tregs. Future studies incorporating wild-type controls and using labeled regulatory cells to track their trafficking to lymphoid tissues and graft sites will help refine our understanding of MDSC-mediated tolerance and tissue-specific immune modulation.

Conclusion

In summary, our study demonstrates that repeated alum administration effectively induces the expansion of immature, suppressive MDSCs and simultaneously activates regulatory T cells (Tregs), resulting in prolonged corneal allograft survival in mice. While MDSCs alone exhibit partial immunosuppressive effects, their combination with Tregs significantly enhances graft tolerance, highlighting a synergistic mechanism. Notably, alum outperforms adoptive MDSC transfer by not only expanding MDSCs but also promoting Tregs activation and inhibiting Th1/Th17 responses. These findings provide new insights into the immunomodulatory properties of alum and support its potential as an immune-conditioning agent in transplantation. Future studies should further explore alum's mechanisms and its applicability to other transplant models or immune-mediated diseases.

Methods

Mice and drug administration

Male BALB/c (H-2d) and C57BL/6 (H-2b) mice, aged 6 to 8 weeks, were purchased from the Institute of Zoology, Chinese Academy of Sciences. Alum (Sigma-Aldrich) or saline (100 μL) was administered intraperitoneally (IP) once daily for 7 consecutive days. The dose and duration were selected based on preliminary studies. This study was approved by the Institutional Animal Care and Use Committee, and all procedures adhered to the ARVO Statement for the Use of Animals in Ophthalmic and Vision Research. Mice were euthanized using carbon dioxide inhalation followed by cervical dislocation, in accordance with institutional and AVMA guidelines. This study is reported in accordance with the ARRIVE guidelines.

Antibodies and flow cytometry (FACS)

For fluorescence-activated cell sorting (FACS) analysis, the following antibodies were used: anti-CD4-APC, anti-CD25-PerCP5.5, anti-CD40L-PE, anti-CTLA-4-PE, anti-CD62L-PE, anti-CD69-PE, anti-PD-1-PE, anti-PD-L1-PE, anti-Gr1-PerCP5.5, anti-Ly6C-PE, anti-CD40-PE, anti-CD80-PE, anti-CD86-PE, anti-TLR2-PE, anti-TLR4-PE, and anti-MHC-II-PE, along with their respective isotype controls (eBioscience, San Diego, CA, USA). For intracellular staining, cells were fixed and permeabilized using Fix/Perm buffer according to the manufacturer's instructions. The following antibodies were used for intracellular staining: Foxp3-FITC, IL-10-PE, IL-2-FITC, IFN-γ-PE, and IL-17 A-PE (eBioscience). Single-cell suspensions were analyzed using a FACScalibur flow cytometer (Becton Dickinson), and data were processed using FlowJo 10 software (Tree Star). Cells were first gated on forward and side scatter (FSC vs. SSC) to identify lymphocytes and exclude debris. Singlets were selected using FSC-H vs. FSC-A plots. To exclude dead cells, a viability gate was applied using Annexin V and 7-AAD double staining, with Annexin V^-/7-AAD^- cells considered viable. Live $CD3^+$ T cells were further gated to identify $CD4^+CD25^+$ regulatory T cells. For MDSC analysis, $CD11b^+Gr\text{-}1^+$ cells were gated from the myeloid compartment.

Proliferation and suppression assays

Suppression assays were performed in triplicate in 96-well round-bottom plates. Freshly isolated naïve $CD4^+$ T cells (1×10^5 cells per well) were labeled with 0.5 μM CFSE (Invitrogen, Molecular Probes) in pre-warmed PBS and incubated at 37 °C for 10 min in the dark. The staining reaction was quenched by adding five volumes of cold complete RPMI-1640 medium supplemented with 10% fetal bovine serum, followed by three washes with PBS to remove excess dye. CFSE-labeled T cells were then stimulated with anti-CD3/CD28 monoclonal antibodies and co-cultured with $CD11b^+$ cells at indicated ratios for 72 h. T cell proliferation was evaluated by flow cytometric analysis of CFSE dilution.The percentage of suppression was calculated using the formula:

Suppression (%) = T cells without MDSCs(T cells without MDSCs)−(T cells with MDSCs)×100%.

Suppression of $CD4^+CD25^-$ T cell activation

$CD4^+CD25^-$ T cells were isolated from the spleens and lymph nodes of naïve C57BL/6 mice using a $CD4^+CD25^+$ Treg isolation kit (Miltenyi Biotec). The purity of the sorted cells was > 90%, as confirmed by flow cytometry. $CD4^+CD25^-$ T cells (1×10^5) were stimulated with anti-CD3/CD28 mAb-coated Dynabeads (1:1 ratio) in the presence or absence of $CD11b^+$ cells (1×10^5) in 96-well flat-bottom plates for 48 h. Surface markers of T cell activation, including CD25, PD-1, CD69, PD-L1, CD62L, CTLA-4, and the nuclear transcription factor Foxp3, were analyzed.

Corneal transplantation

A standard murine orthotopic corneal transplantation model was used as described previously[14]with minor modifications. Briefly, 2-mm central corneal grafts from BALB/c mice were excised and sutured onto 2-mm recipient graft beds in the central corneas of C57BL/6 mice. Graft status was evaluated weekly using slit-lamp biomicroscopy. Grafts were considered rejected when they became opaque, and iris details were no longer visible,

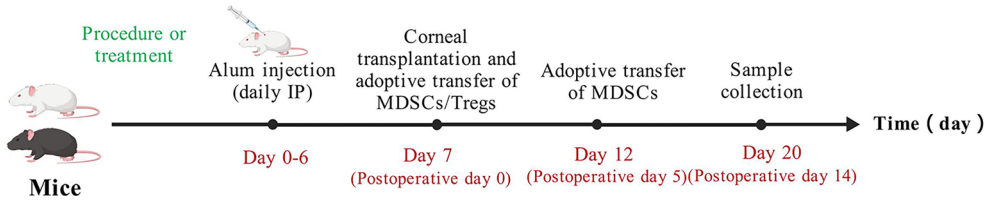

Fig. 7. The schematic diagram illustrating the experimental timepoints and cell administration procedures.

according to a standardized opacity grading scale (0–5). The experimental groups included recipients treated with alum, adoptive transfer of MDSCs, or co-transfer of MDSCs and Tregs. PBS-treated allograft recipients served as positive controls, while syngeneic graft recipients served as negative controls.

Adoptive transfer

Alum-treated mice were sacrificed, and $CD11b^+$ cells were isolated from spleens and bone marrow using a $CD11b^+$ isolation kit (Miltenyi Biotec). The purity of $CD11b^+Gr1^+$ cells was confirmed to be >90% via flow cytometry. $CD11b^+$ cells (2×10^6 per mouse) were intravenously transferred to allograft recipients on postoperative days 0 and 5. $CD4^+CD25^+$T cells (Tregs)were isolated from the spleens and lymph nodes (LNs) of Alum-treated mice using a $CD4^+CD25^+$ regulatory T cell isolation kit (Miltenyi Biotec, Germany). The purity of the isolated cells was confirmed by flow cytometry and found to be greater than 90%. Treg cells (1×10^6 per mouse) were intravenously transferred to allograft recipients on postoperative days 0. Allograft survival ($n=10$ per group) was monitored for up to five weeks. Draining submandibular lymph nodes were harvested at day 14 post-surgery for analysis of Foxp3, IL-10, IL-2, IFN-γ, and IL-17 A expression. A schematic diagram illustrating the experimental timeline and cell administration procedures has been shown as Fig. 7.

Statistical analysis

Statistical analyses were performed using SPSS 13.0. A Student's *t*-test was used for pairwise comparisons, while one-way ANOVA was used for multiple comparisons. Graft survival was analyzed using the Kaplan-Meier method with a Mantel-Cox log-rank test. Data are presented as mean ± SD, and $P<0.05$ was considered statistically significant.

Data availability

The datasets generated and/or analyzed during the current study are available from the corresponding author upon reasonable request.

Received: 29 May 2025; Accepted: 16 July 2025
Published online: 21 July 2025

References

1. Veglia, F., Sanseviero, E. & Gabrilovich, D. I. Myeloid-derived suppressor cells in the era of increasing myeloid cell diversity. *Nat. Rev. Immunol.* **21**, 485. https://doi.org/10.1038/s41577-020-00490-y (2021).
2. Cuenca, A. G. et al. A paradoxical role for myeloid-derived suppressor cells in sepsis and trauma. *Mol. Med.* https://doi.org/10.2119/molmed.2010.00178 (2011).
3. Lasser, S. A., Ozbay Kurt, F. G., Arkhypov, I., Utikal, J. & Umansky, V. Myeloid-derived suppressor cells in cancer and cancer therapy. *Nat. Rev. Clin. Oncol.* **21**(2), 147–164. https://doi.org/10.1038/s41571-023-00846-y (2024).
4. Ma, T. et al. Myeloid-derived suppressor cells in solid tumors. *Cells* **11**(2), 310. https://doi.org/10.3390/cells11020310 (2022).
5. Schrijver, I. T., Théroude, C. & Roger, T. Myeloid-derived suppressor cells in sepsis. *Front. Immunol.* **10**, 327. https://doi.org/10.3389/fimmu.2019.00327 (2019).
6. Bekić, M. & Tomić, S. Myeloid-derived suppressor cells in the therapy of autoimmune diseases. *Eur. J. Immunol.* **53**(12), e2250345. https://doi.org/10.1002/eji.202250345 (2023).
7. Cao, P. et al. Myeloid-derived suppressor cells in transplantation tolerance induction. *Int. Immunopharmacol.* **83**, 106421. https://doi.org/10.1016/j.intimp.2020.106421 (2020).
8. Ge, J. et al. Adjuvant conditioning induces an immunosuppressive milieu that delays alloislet rejection through the expansion of myeloid-derived suppressor cells. *Am. J. Transplant.* **23**(7), 935–945. https://doi.org/10.1016/j.ajt.2023.04.015 (2023).
9. Shao, L. et al. Emerging role of myeloid-derived suppressor cells in the biology of transplantation tolerance. *Transplantation* **104**(3), 467–475. https://doi.org/10.1097/TP.0000000000000299610 (2020).
10. Lee, S. et al. Myeloid-derived suppressor cells promote allograft survival by suppressing regulatory T cell dysfunction in high-risk corneal transplantation. *Am. J. Transplant.* **24**(9), 1597–1609. https://doi.org/10.1016/j.ajt.2024.03.022 (2024).
11. Ren, Y. et al. Myeloid-derived suppressor cells improve corneal graft survival through suppressing angiogenesis and lymphangiogenesis. *Am. J. Transplant.* **21**(2), 552–566. https://doi.org/10.1111/ajt.16291 (2021).
12. Ren, Y. et al. Rapamycin antagonizes angiogenesis and lymphangiogenesis through myeloid-derived suppressor cells in corneal transplantation. *Am. J. Transplant.* **23**(9), 1359–1374. https://doi.org/10.1016/j.ajt.2023.05.017 (2023).
13. Zhu, J. et al. Ex vivo-induced bone marrow-derived myeloid suppressor cells prevent corneal allograft rejection in mice. *Invest. Ophthalmol. Vis. Sci.* **62**(7), 3. https://doi.org/10.1167/iovs.62.7.3 (2021).
14. Guo, X. et al. In vitro-expanded CD4(+)CD25(high)Foxp3(+) regulatory T cells control corneal allograft rejection. *Hum. Immunol.* **73**(11), 1061–7. https://doi.org/10.1016/j.humimm.2012.08.014 (2012).
15. Gabrilovich, D. I. Myeloid-derived suppressor cells. *Cancer Immunol. Res.* **5**(1), 3–8. https://doi.org/10.1158/2326-6066.CIR-16-0297 (2017).

16. Nourbakhsh, E., Mohammadi, A., Salemizadeh Parizi, M., Mansouri, A. & Ebrahimzadeh, F. Role of myeloid-derived suppressor cell (MDSC) in autoimmunity and its potential as a therapeutic target. *Inflammopharmacology* **29**(5), 1307–1315. https://doi.org/10.1007/s10787-021-00846-3 (2021).
17. Scalea, J. R., Lee, Y. S., Davila, E. & Bromberg, J. S. Myeloid-derived suppressor cells and their potential application in transplantation. *Transplantation* **102**(3), 359–367. https://doi.org/10.1097/TP.0000000000002022 (2018).
18. Magcwebeba, T., Dorhoi, A. & du Plessis, N. The emerging role of myeloid-derived suppressor cells in tuberculosis. *Front. Immunol.* **30**(10), 917. https://doi.org/10.3389/fimmu.2019.00917 (2019).
19. Malavika, M. et al. Role of myeloid-derived suppressor cells in sepsis. *Int. Immunopharmacol.* **104**, 108452. https://doi.org/10.1016/j.intimp.2021.108452 (2022).
20. Joshi, S. & Sharabi, A. Targeting myeloid-derived suppressor cells to enhance natural killer cell-based immunotherapy. *Pharmacol. Ther.* **235**, 108114. https://doi.org/10.1016/j.pharmthera.2022.108114 (2022).
21. Kim, W. et al. PD-1 signaling promotes tumor-infiltrating myeloid-derived suppressor cells and gastric tumorigenesis in mice. *Gastroenterology* **160**(3), 781–796. https://doi.org/10.1053/j.gastro.2020.10.036 (2021).
22. Zhao, T. et al. LAL deficiency induced myeloid-derived suppressor cells as targets and biomarkers for lung cancer. *J. Immunother. Cancer* **11**(3), e006272. https://doi.org/10.1136/jitc-2022-006272 (2023).
23. Zhou, L. X. et al. Myeloid-derived suppressor cells-induced exhaustion of CD8+ T cells participates in rejection after liver transplantation. *Cell Death Dis.* **15**(7), 507. https://doi.org/10.1038/s41419-024-06834-z (2024).
24. Han, D., Tao, J., Fu, R. & Shao, Z. Myeloid-derived suppressor cell cytokine secretion as prognostic factor in myelodysplastic syndromes. *Innate Immun.* **26**(8), 703–715. https://doi.org/10.1177/1753425920961157 (2020).
25. Yin, B., Cai, Y., Chen, L., Li, Z. & Li, X. Immunosuppressive MDSC and Treg signatures predict prognosis and therapeutic response in glioma. *Int. Immunopharmacol.* **141**, 112922. https://doi.org/10.1016/j.intimp.2024.112922 (2024).
26. Khalaf, K. et al. Aspects of the tumor microenvironment involved in immune resistance and drug resistance. *Front. Immunol.* **12**, 656364. https://doi.org/10.3389/fimmu.2021.656364 (2021).
27. Lauder, S. N. et al. Treg-driven tumour control by PI3Kδ inhibition limits myeloid-derived suppressor cell expansion. *Br. J. Cancer* **127**(9), 1595–1602. https://doi.org/10.1038/s41416-022-01917-0 (2022).
28. Luan, Y. et al. Monocytic myeloid-derived suppressor cells accumulate in renal transplant patients and mediate CD4+ Foxp3+ Treg expansion. *Am. J. Transplant.* **13**(12), 3123–31. https://doi.org/10.1111/ajt.12461 (2013).
29. Miyairi, S. et al. Donor bone marrow cells are essential for iNKT cell-mediated Foxp3+ Treg cell expansion in a murine model of transplantation tolerance. *Eur. J. Immunol.* **47**(4), 734–742. https://doi.org/10.1002/eji.201646670 (2017).

Acknowledgements

This work was supported by the Science and Technology Department of Shanxi Province, Shanxi Provincial Basic Research Program Project, 202403021221314; Changzhi Medical College 2024 Annual Doctoral Research Start-up Fund Project,2024BS10.

Author contributions

L.L. and Y.H. conceived and designed the study. D.R. and Y.Z. performed the animal experiments and flow cytometry. X.X. analyzed the data and prepared the figures. X.G. contributed to manuscript writing and data interpretation. S.H. supervised the project and critically revised the manuscript. All authors reviewed and approved the final version of the manuscript.

Declarations

Competing interests

The authors declare no competing interests.

Additional information

Supplementary Information The online version contains supplementary material available at https://doi.org/10.1038/s41598-025-12289-9.

Correspondence and requests for materials should be addressed to S.H. or X.G.